

## Solar Polarimetry: An Overview

H. Lin

*Institute for Astronomy, University of Hawaii*  
*Kula, Hawaii 96790, USA*

**Abstract.** Polarimetry has many applications and a long history in solar physics research. The first polarimetric observation of a sunspot was performed by G. E. Hale in 1908. Today, polarimetry is one of the most important diagnostic tools of solar astronomy. The presence of solar magnetic fields naturally produces many polarized spectral lines that are useful for the study of solar magnetism. In addition, the scattering process and the interaction between the magnetic field and the scattering process yield additional important diagnostic tools for studies of solar phenomena and physical processes that are otherwise difficult to observe. This review describes how these polarimetric diagnostics are being utilized in our endeavor to achieve a comprehensive understanding of the Sun.

### 1. Introduction

#### 1.1. Polarization Mechanisms in Solar Physics

Polarized radiation arises naturally in the solar atmosphere through several polarization mechanisms. The strongest polarized solar radiation originates from sunspots and active regions with intense magnetic fields via the *Zeeman effect*. In these regions, magnetic fields modify the absorption coefficients of magnetically sensitive spectral lines to produce strongly polarized absorption spectra. Without magnetic fields, solar radiation would be polarized only weakly by scattering processes. When observing the Sun near the limb, scattering of anisotropic photospheric illumination by atoms in the upper photosphere produces a weak but rich linear polarization spectrum (the second solar spectrum) that has many interesting new applications in quantum physics. In the corona, as the anisotropy factor increases with height, the magnitude of the scattering polarization is also higher, and polarimetric observations of the continuum polarization due to Thomson scattering by the electrons are commonly used to distinguish the solar corona from the glaring telescopic scattered light from the photosphere.

In the upper atmosphere of the Sun, *magnetic resonant scattering* is primarily responsible for the polarization of the spectral lines. In the presence of a magnetic field, the polarization of the scattered radiation by the neutral atoms and ions is strongly modulated by the magnetic fields. However, the response of the polarization signals to the magnetic fields depends on the nature of the atomic transition involved in the scattering processes. In the upper photosphere, *Hanle effect* polarization can be used for the study of turbulent photospheric magnetic fields. In the corona, polarimetry of the magnetic resonant scattering off the for-

bidden coronal emission lines can be used for direct measurement of the coronal magnetic fields. These processes will be described in more detail in §§ 2 and 3.

## 1.2. Instrumentation and Techniques for Solar Polarimetry

While polarimetry offers diverse and important diagnostics for the study of the Sun, utilization of these diagnostics is not trivial. Because of the wide-ranging physical parameters involved in the polarization processes, the amplitudes of the polarization signals range from almost 100% in strong photospheric magnetic features to  $10^{-4}$  or less in the solar corona. Precise measurements of these polarization signals requires carefully designed instrumentation and observing techniques to minimize spurious polarization signals that may arise from non-ideal observing conditions and telescope optics.

Interestingly, even with the early recognition of the importance of polarimetry in solar physics, most of the existing large-aperture general purpose solar telescopes (e.g., the Dunn Solar Telescope and the McMath-Pierce Solar Telescope of the U.S. National Solar Observatory, or the Swedish Solar Telescope in La Palma) were not optimized for polarimetric observations.<sup>1</sup> The optics of these telescopes that are used for tracking the movement of the Sun across the sky generate strong time-varying polarization crosstalk that may render the polarimetry data unusable if not properly corrected. To cope with the precision required for polarimetric observations, solar astronomers have developed a large array of specialized instrumentation, as well as observation and polarization calibration techniques. Because polarization of solar radiation can occur in disparate environments involving many different atomic species, tremendous theoretical efforts have been devoted to obtaining a detailed understanding of the polarization mechanisms in the solar atmosphere so that observations can be interpreted in a meaningful way. Today, solar astronomers routinely observe polarization signals with high time and spatial resolution and/or with very low amplitude—all in the presence of very large background signals and systematic errors—to study a large variety of solar phenomena.

Since the instrumentation and techniques for polarization analysis used in solar observations are fundamentally the same as those used in nighttime observations, we will not cover this subject in great detail, but refer readers to the excellent review by Hough (2004). Nevertheless, solar observations do have very stringent polarimetric requirements, and as a result, solar astronomers have developed specialized polarimetric equipment to meet these requirements. Some examples are the C3PO detector concept described by Keller (2004) and the ZIMPOL instrument described by Schmid et al. (2004). Techniques to calibrate and correct telescope and instrumental polarization crosstalk can be found in Skumanich et al. (1997) and Kuhn et al. (1994).

Technologies developed during the past two decades have made it possible to conduct polarimetry observations with ultra-high sensitivity, and have created new research opportunities. The most prominent among these exciting new

---

<sup>1</sup>The first attempt to build a “polarization-free” solar telescope was the 2.4 m LEST (Large Earth-based Solar Telescope) project, which did not materialize. The French-Italian Themis (<http://www.themis.iac.es>) is a 90 cm aperture polarization-free solar telescope specifically designed for visible polarimetric measurements of photospheric vector magnetic fields.

developments is perhaps the discovery of the second solar spectrum (Stenflo et al. 1983a), and the new capability to measure the coronal magnetic fields directly (Lin et al. 2000, 2004). With the prominent role of polarimetry in modern solar physics research and the tremendous amount of work that is currently being done in this field, it is obviously impossible to attempt a thorough review of the subject in a short article. Therefore, this article will provide only an abbreviated summary of the current research subjects in solar physics using polarimetric techniques. Interested readers can find detailed discussions of specific subjects in the references cited.

## 2. Polarimetry in the Photosphere

In the solar photosphere, gas pressure dominates magnetic pressure, and magnetic fields are found in concentrated form such as sunspots and network magnetic field elements with field strength greater than 1000 G. However, even during solar maximum, these strongly magnetized areas only account for a small fraction of the solar surface. Because of the high conductivity of the solar plasma, the vigorous convective motions of solar granulation may act as small-scale dynamos to generate turbulent magnetic fields. Indeed, outside of the the kilogauss-field regions, a weak-field component with a broad field strength distribution (below 1000 G) can be found everywhere on the surface of the Sun. The stronger of these weak fields appear to be clustered in the intergranular lanes (*granular magnetic fields*, Lin & Rimmele 1999), and evolve with a timescale comparable to the lifetime of the solar granulations. Very weak fields with spatial scale and flux density below the current detection limit are also expected to exist everywhere in the photosphere. How photospheric magnetic fields are organized into different structures with size and field strength spanning over several order of magnitudes is still not well understood, and polarimetry is the most important tool for the study of these fascinating phenomena.

### 2.1. Zeeman Effect Diagnostics of Photospheric Magnetic Fields

The primary polarization mechanism in the photosphere is the Zeeman effect. This is perhaps the most well-known polarization mechanism on the Sun, and it has been extensively studied (e.g., Jefferies et al. 1989, and references therein) and used since the beginning of modern solar magnetic field research.

*Sunspot Magnetic Fields* Sunspots are large, long-lived magnetic structures with field strength in the umbra reaching 2000 to 3000 G. They are considered to be the surface manifestation of the strong magnetic fields generated by the solar dynamo operating at the base of the convection zone. Although the sunspot phenomenon can be understood conceptually by considering a simple, monolithic magnetic flux tube in magnetohydrostatic equilibrium with the surrounding “nonmagnetic” plasma, many aspects of the sunspot phenomenon at small scales remain unexplained. High-resolution images of sunspots have revealed that sunspots consist of many small-scale (subarcsecond) features. Understanding the magnetic properties of these small-scale features is key to understanding the physics of sunspots.

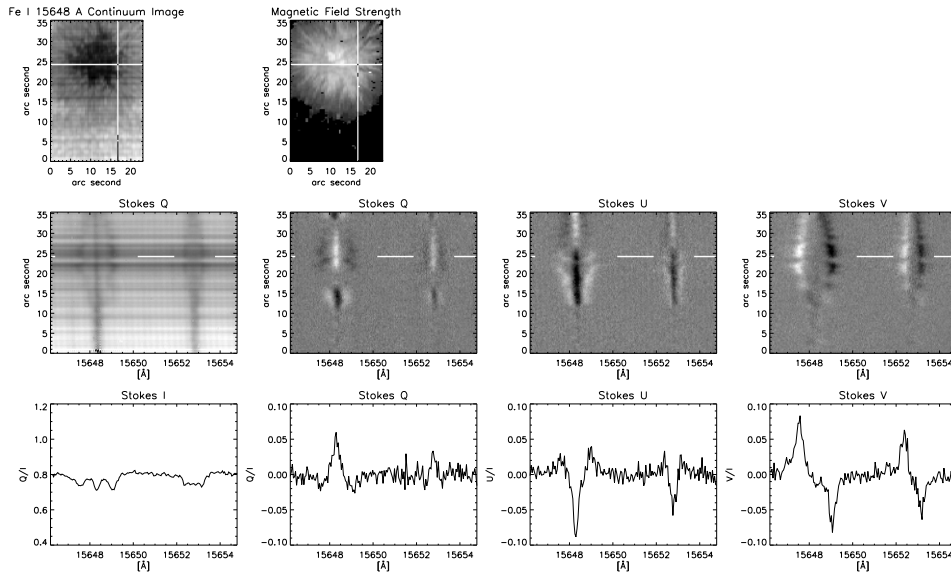


Figure 1. Examples of high-resolution full Stokes spectra of a sunspot obtained with an adaptive optics system.

Figure 1 shows an example of high-resolution polarized Zeeman effect sunspot spectra of the FeI 1564.8 nm and FeI 1565.3 nm line pair obtained with an adaptive optics system. The effective Lande factors of the two lines are  $g = 3$  and  $g = 1.5$ , respectively. Since the magnetic filling factor is close to 1 inside sunspots, the spectral lines are almost 100% polarized. Because of the high magnetic field strength ( $\sim 2500$  G), the components of the Zeeman triplet are completely resolved. Thus, the three components of the magnetic field vector (field strength, inclination, and azimuthal angles) can be determined (subject to a  $180^\circ$  ambiguity). Many inversion techniques (e.g., Skumanich & Lites 1987; Westendorp Plaza et al. 1998) have been devised to derive the vector magnetic field configuration of the sunspot magnetic fields from measurements of full Stokes spectra like those in Figure 1, with some of them also attempting to derive the height variations of the the magnetic fields. Examples of 3-D sunspot magnetic field structure measurements can be found in, e.g., Westendorp Plaza et al. (2001) and Mathew et al. (2003). Current efforts are focused on obtaining high-resolution polarimetric observations to understand the small-scale structure of sunspots.

*Quiet-Sun Magnetic Fields* What's the origin of the weak quiet-Sun magnetic fields? Are they the fundamental building blocks of the solar surface magnetic fields with kilogauss field strength? Observations of the magnetic fields in the quiet Sun are difficult because the small-scale magnetic field features produce only very weak polarization signals that can easily be overwhelmed by spurious polarization signals caused by poor observing conditions and/or instrumental effects. However, significant progress has been made in this field in the past 10 years. Figure 2 shows examples of precision quiet-Sun Stokes  $V$  spectra that demonstrates the weak and random nature of the quiet-Sun magnetic

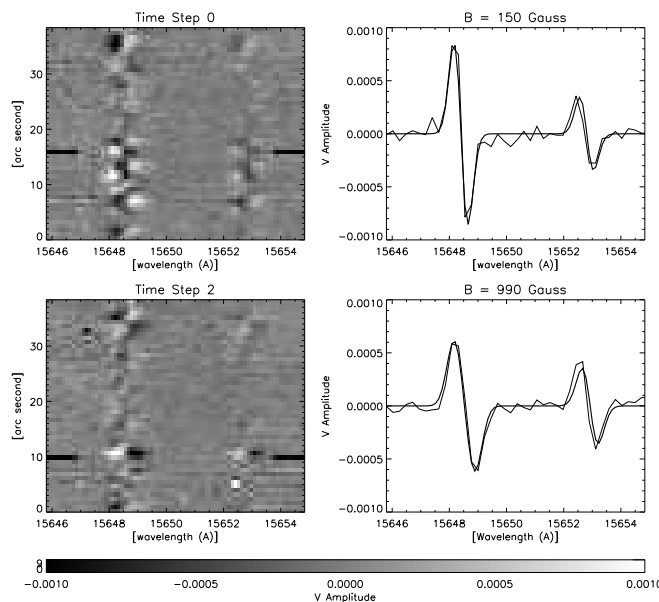


Figure 2. Examples of quiet-Sun Stokes  $V$  spectra.

fields. From spectra like these, Lin (1995) and Lin & Rimmele (1999) were able to demonstrate that the distribution of solar surface magnetic fields can be described by a bimodal distribution, and now it is generally agreed that the quiet-Sun magnetic fields are likely to be generated and supported by a small-scale dynamo associated with the granulation convective flow, which is distinctively different from the larger flux tubes of network magnetic fields, pores, and sunspots.

## 2.2. Photospheric Scattering Polarization

*The Second Solar Spectrum* One of the most interesting recent developments in solar astrophysics is the discovery of the second solar spectrum (Stenflo et al. 1983a,b). When observing the Sun with a polarimetric sensitivity of  $10^{-4}$  or lower, the whole solar spectrum is linearly polarized even without the presence of magnetic fields by scattering processes. Because the atomic transition of every spectral line is different, a large array of polarization effects involving processes such as quantum interference, hyperfine structure, optical pumping, isotope effects, and signature of rare elements is produced. The second solar spectrum was the subject of a series of solar polarization workshops (Stenflo & Nagendra 1996; Nagendra & Stenflo 1999; Trujillo Bueno & Sanchez Almeida 2003), and a two-volume atlas is now available (Gandorder 2000, 2002).

Figure 3 shows the linearly polarized spectrum of the Ca II H and K line spectrum observed near the solar limb (Stenflo 1980) that demonstrates the fascinating physical processes involved in the second solar spectrum. The intrinsic polarizability  $W_2$  of a scattering event depends on the total angular momentum of the transition (Stenflo 1994). For the Ca II K line,  $W_2 = 0.5$ , and for the Ca II H line,  $W_2 = 0$ , which means that the Ca II H line is intrinsically not polarizable. However, contrary to the theoretical prediction, the linear polarized spectrum

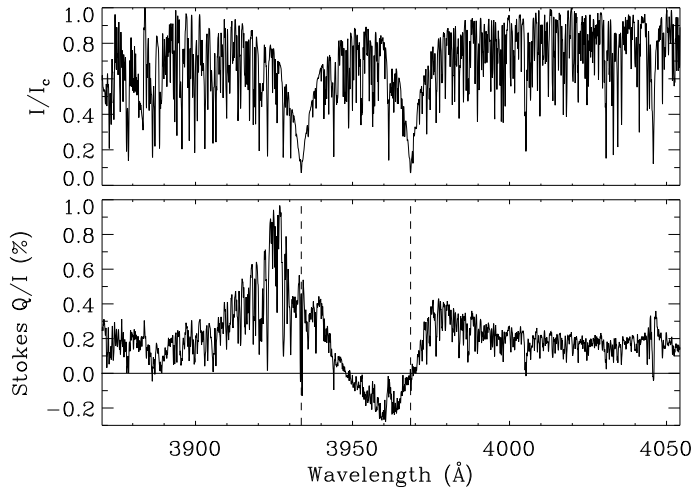


Figure 3. The linearly polarized spectrum of the Ca II H and K line. Courtesy of J. O. Stenflo.

of the Ca II H line has a intriguing spectral profile with sign reversal around the center of the line. This phenomenon is due to the quantum interference between the Ca II H and K states, and has been successfully modeled (Auer et al. 1980; Stenflo 1980).

The second solar spectrum is full of surprises like this and many other interesting scattering polarization phenomena. A recent review of these subjects is provided by Stenflo (2004).

*Hanle Effect Diagnostics of Turbulent Magnetic Fields* For magnetically sensitive photospheric spectral lines, their polarization spectra induced by the scattering process are modified by the magnetic fields. This phenomenon is usually referred to as the Hanle effect. The main consequences of the Hanle effect are the depolarization (decrease in the degree of linear polarization) of the spectral line and the rotation of the direction of the linear polarization. Since the Hanle effect is effective only in the regime where the magnetic field is weak such that the Zeeman splitting of the magnetic substates is small compared with the natural linewidth of the spectral line and that the depolarizing effect is insensitive to the sign of the magnetic field, it has great utility for diagnosing the turbulent magnetic fields (Faurobert et al. 2001; Shchukina & Trujillo Bueno 2003).

### 3. Polarimetry of the Solar Corona

Due to the high temperature conditions, the coronal plasma is highly ionized. Nevertheless, regions of cool and dense neutral plasma (*prominences* and *filaments*) can exist amid the hot environment, typically above the neutral lines between large photospheric bipolar regions. The density of the corona is many orders of magnitude lower than the photosphere, and the dominant source of radiation in the visible and near-IR wavelengths is the scattering of the bright

photospheric radiation off the electrons and neutral and ionized atoms. The radiation of the solar corona is polarized by the scattering processes, as well as by the interaction between the magnetic fields and the scattering processes. Thus, many interesting polarimetric diagnostics tools can be used for the study of the solar corona. Significant progress has been made in recent years, and this section gives an overview of how polarimetry is helping us better understand the physics of the solar corona.

### 3.1. Polarimetric Observations of the K Corona

Observations of the solar corona outside of eclipse are difficult because of the low surface brightness of the emission of the corona. Even with a coronagraph located at a high-altitude site with dark sky conditions, the strength of coronal emissions is not much higher than the brightness of the daytime sky or the instrumental scattered light. However, the daytime sky (forward scattering of sunlight by Earth's atmosphere) within a few degrees of the line of sight to the Sun is not strongly polarized, nor is instrumental scattered light produced within the telescope. Therefore, broadband polarimetric observations can be used to discern the faint coronal emission from the bright sky and instrumental scattered light. The coronal photometer (Smartt 1982) of the Evans Solar Facilities of the National Solar Observatory at Sacramento Peak, New Mexico, and the K-coronameter (Chalmers 1985) of the High Altitude Observatory are two such instruments. Space-based coronagraphs, such as LASCO (Large Angle and Spectrometric Coronagraph) instruments on board SOHO (Solar and Heliospheric Observatory), also employ polarimetric techniques to better isolate the coronal emission from the instrumental scattered light.

### 3.2. Hanle Effect of Prominences and Filaments

Prominences and filaments are regions of the solar corona containing cool ( $10^5$  K) and dense materials embedded in otherwise hot ( $10^6$  K) and tenuous surroundings. They are most prominent in images taken in the core of strong solar lines such as H $\alpha$  and He I 1083.0 nm lines. Exactly how these islands of cool materials form and persist is still not clear, although magnetic support is generally accepted as the most viable explanation (Kuperus & Raadu 1974; Kippenhahn & Schluter 1975).

*He I D3 Observations of Prominences* The magnetic fields of the prominences were measured by the Hanle effect of the He I D3 line (Leroy 1989; Casini et al. 2003). The theory of the He I D3 Hanle effect polarization has been extensively studied by many authors (e.g. Bommier et al. 1994, and references therein). When observing He I D3 on the limb, prominences appear as emission features against the dark sky background. The anisotropic resonant scattering of the photospheric radiation produces a linear polarization parallel to the local solar limb with its amplitude increasing with the height of the scattering atoms. Magnetic fields reduce the degree of linear polarization (depolarization) and/or rotate the orientation of the linear polarization. The circular polarization depends on the longitudinal magnetic fields, similar to the Zeeman effect. This line is optically thin and cannot be seen as absorption features (filaments) on the solar disk.

*He I 1083.0 nm Observations of Filaments* Similar to  $H\alpha$  observations, prominences appear as dark absorption features (filaments) on the solar disk in He I 1083.0 nm line. Filament polarization observations have several advantages. First, filaments can be tracked over a two-week period as they rotate across the visible solar disk. Observations with different scattering geometry potentially can be used to resolve ambiguities inherent in limb prominence observations due to line-of-sight integration. Also, disk Hanle effect observation is not subject to the  $180^\circ$  ambiguity, and the orientation of the magnetic field vector can be uniquely determined. The first He I 1083.0 nm polarization map of a filament was obtained by Lin et al. (1998), which also revealed interesting atomic polarization effects (Trujillo Bueno et al. 2002).

### 3.3. Polarization of Forbidden Coronal Emission Lines

Magnetic fields dominate the structure and dynamics of the solar corona. Despite its importance, there are no reliable direct coronal magnetic field observations, and solar physicists rely on proxy measurements such as UV emission line images to infer the magnetic field structure of the corona. Numerical extrapolation from photospheric magnetic field observations are also extensively used to model the coronal fields (Lee et al. 1999; Roussev et al. 2003). These extrapolations are fundamentally limited by the difficulty of extrapolating between regions where force-free and non-force-free conditions apply. The extrapolation process is also an ill-posed boundary value problem in which minute errors in the data grow exponentially (Low & Lou 1990). Physical models of the corona ultimately rest on direct magnetic field observations.

Among the various techniques for the measurement of coronal magnetic fields, the observation of the forbidden coronal emission line (CEL) polarization profile is the most powerful and promising. The polarization of the forbidden CELs arises from *incoherent* resonance scattering of photospheric radiation by the highly ionized coronal atoms in the presence of a magnetic field (House 1977; Casini & Judge 1999; Lin & Casini 2000). The orientation of the CEL linear polarization maps the direction of the coronal magnetic field projected on the plane of the sky (subject to a  $90^\circ$  ambiguity), while the circular polarization measures the strength (flux) of the magnetic field. Therefore, by measuring the full Stokes polarization state of the CEL, we can, in principle, determine the magnetic field configuration of the solar corona.

The polarimetric response of the forbidden CEL (such as Fe XVI 530.0 nm, Fe XIII 1074.7 nm) to the magnetic field is drastically different from that of the permitted transitions (e.g.,  $H\alpha$ , He I D3 580.0 nm, He I 1083.0 nm) for atoms in the cool and dense prominences and filaments discussed in the previous section (§3.2.), despite identical scattering geometry. The difference in the polarimetric response is due to the different coherency properties between the magnetic substates. For the forbidden CELs (usually magnetic dipole [M1] transition), the Einstein spontaneous emission coefficient  $A$  of the transition is very small, typically  $\sim 10 \text{ s}^{-1}$ . Therefore, the natural linewidths of these CELs are very small compared with the Zeeman frequency splitting even when the magnetic field is very weak, and the condition  $\omega_B \gg A$  (where  $\omega_B$  is the Larmor frequency) is always satisfied. In this condition, the magnetic substates separated by  $\omega_B$  do not interfere with each other, and they evolve *incoherently*. In contrast, the

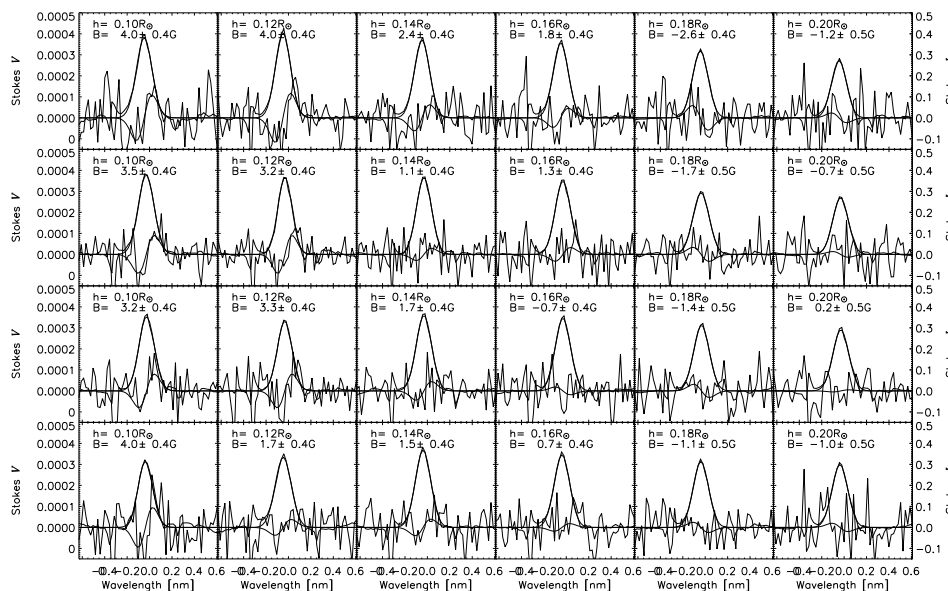


Figure 4. Stokes  $V$  spectra from a  $120'' \times 80''$  region in the corona above active region NOAA 0581 obtained on the west limb of the Sun. Geographical north (east) is at the top (left) of the figure.

magnetic substates of permitted lines (electric dipole [E1] transition) interfere strongly with each other due to their broad natural linewidth (large  $A$  coefficient) under weak field conditions, and they evolve *coherently*. Details about how the quantum interference leads to the different polarimetric properties of the E1 and M1 transitions are discussed in Lin & Casini (2000).

The amplitudes of the CEL linear polarization signals are expected to be a few percent of the background continuum (due to sky and instrumental scattered light) at a height of  $0.05 R_{\odot}$ , and increase with height, and are easily measured (Mickey 1973; Arnaud 1987; Habbal et al. 2000). However, the amplitude of the CEL circular polarization signal due to the Zeeman effect is expected to be at the  $10^{-4} \times I_c$  level or lower. Although with fast modern array detectors and polarimeters, ultra-high-sensitivity polarimetry measuring polarization signals at the  $10^{-4} \times I_c$  level can be obtained routinely from the photosphere with reasonable integration times ( $\approx$  minutes), the low photon flux of the solar corona and the lack of a large aperture coronagraph make the observation of the circular polarization due to coronal magnetic fields extremely difficult. Only a few measurements were attempted (Harvey 1969; Kuhn 1995), and Lin et al. (2000) was the first group to obtain a definitive measurement of the magnetic Stokes  $V$  profile of the Fe XIII 1074.7 nm line.

Although Lin et al. have demonstrated the feasibility of CEL polarimetry as a diagnostic for the coronal magnetic fields, measurements with two-dimensional spatial coverage are needed to resolve the structure of coronal magnetic fields. Furthermore, time series are required for the study of the evolution of the coronal magnetic field structures during energetic eruptive events such as flares and coro-

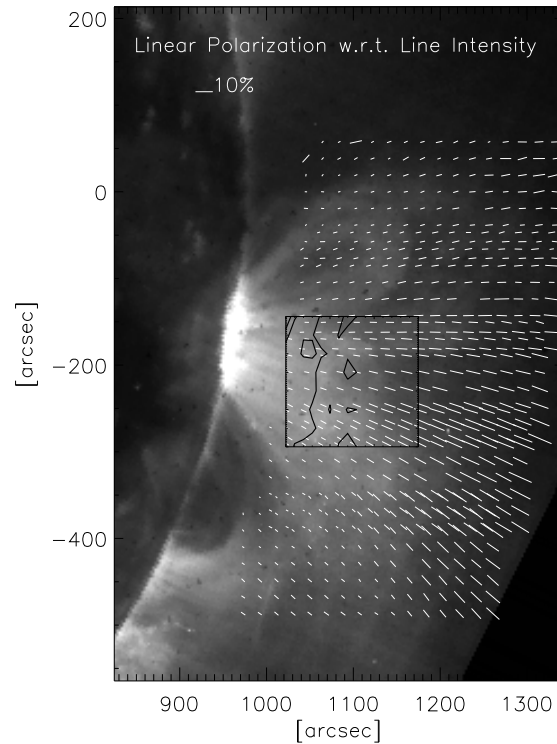


Figure 5. “Vector” magnetogram of the solar corona. The grayscale image is the Fe XII 19.5 nm image from EIT (Extreme Ultraviolet Imaging Telescope) instrument on SOHO. The orientation and magnitude of the linear polarization of the Fe XIII 1074.7 nm coronal emission line are shown by the white lines. The black contours show the magnitude of the line-of-sight magnetic field strength. The orientation the magnetic field projected in the plane of sky can be inferred from the linear polarization map with a  $90^\circ$  ambiguity: it is either parallel or perpendicular to the direction of linear polarization, depending on the angle between the magnetic field vector and the local vertical direction.

nal mass ejections. Using a new optical fiber bundle imaging spectropolarimeter (OFIS, Lin 2004) and a new 50 cm aperture off-axis mirror coronagraph (Kuhn et al. 2003), the first *coronal magnetogram* were obtained recently (Lin et al. 2004). Figure 4 shows the Stokes  $V$  spectra from a  $6 \times 4$  “pixel” ( $20''/\text{pixel}$ ) region from the corona above active region NOAA 0581 during its west limb transit. A 70 min integration time was required to achieve the high (1 G) magnetic field sensitivity. Figure 5 shows the contour of the longitudinal coronal magnetic fields above an active region overplotted on the EIT Fe XII 19.5 nm intensity image and the orientation of the coronal magnetic fields projected in the plane of sky with respect to the intensity structure of the corona. Obviously such data will provide rich new information and help improve our understanding of the solar corona.

#### 4. The Future of Solar Polarimetry

Observations of polarization are differential measurements, so the polarization sensitivity of the observations is essentially limited only by photon statistics. With the rapid advance of several key technologies—including solar adaptive optics (Rimmele 2000) and sensitive and fast array detectors—solar polarimetry has achieved unprecedented sensitivity and precision, and is now only limited by the photon-collecting capability of the existing telescopes. Recognizing the importance of a new large aperture solar telescope for further advancement of solar physics, the U.S. solar community has proposed the construction of a 4 m aperture solar telescope—the Advanced Technology Solar Telescope (ATST, Keil et al. 2003).<sup>2</sup> ATST is optimized for high spatial resolution and high precision and sensitivity polarimetric observations with broad wavelength coverage, and will provide an order of magnitude increase in photospheric and coronal observing capabilities to further advance our understanding of the Sun.

#### References

- Arnaud, J., & Newkirk, G., Jr. 1987, *A&A*, 170, 263  
 Auer, L., Rees, D., & Stenflo, J. O. 1980, *A&A*, 88, 302  
 Bommier, V., Landi Degl'innocenti, E., Leroy, J. L., & Sahal-Brechot, S. 1994, *Solar Phys.*, 154, 231  
 Casini, R., & Judge, P. 1999, *ApJ*, 522, 542  
 Casini, R., López Ariste, A., Tomczyk, S., & Lites, B. W. 2003, *ApJ*, 598, L67  
 Chalmers, J. W. 1985, NCAR Technical Note, TN-247+1A, 17  
 Faurobert, M., Arnaud, J., Vigneau, J., & Frisch, H. 2001, *A&A*, 378, 627  
 Gandorder, A. 2000, *The Second Solar Spectrum*, Vol. I: 4625 Å to 6995 Å (Zurich: VdF)  
 Gandorder, A. 2002, *The Second Solar Spectrum*, Vol. II: 3910 Å to 4630 Å (Zurich: VdF)  
 Habbal, S. R., Woo, R., & Arnaud, J. 2000, *ApJ*, 558, 852  
 Harvey, J. W. 1969, Ph.D. Dissertation, University of Colorado  
 Hough, J. H. 2004, this volume.  
 House, L. L. 1977, *ApJ*, 214, 632  
 Jefferies, J., Lites, B., & Skumanich, A. 1999, *ApJ*, 343, 920  
 Keil, S. L., Rimmele, T., Keller, C. U., Hill, F., Radick, R. R., Oschmann, J. M., Warner, M., Dalrymple, N. E., Briggs, J., Hegwer, S. L., & Ren, D. 2003, *Proc. SPIE*, 4853, 240  
 Keller, C. U. 2004, this volume.  
 Kippenhahn, R., & Schluter, A. 1975, *Astrophys.*, 43, 36  
 Kuhn, J. R. 1995, in *Infrared Tools for Solar Astrophysics: What's Next?*, ed. J. R. Kuhn and M. J. Penn (Singapore: World Scientific), 89  
 Kuhn, J. R., Balasubramaniam, K. S., Kopp, G., Penn, M. J., Dombard, A. J., & Lin, H. 1994, *Solar Phys.*, 153, 143  
 Kuhn, J. R., Coulter, R., Lin, H., & Mickey, D. L. 2003, *Proc. SPIE*, 4853, 318  
 Kuperus, M., & Raadu, M. A. 1974, *A&A*, 31, 189  
 Lee, J., White, S. M., Kundu, M. R., Mickić, Z., & McClymont, A. N. 1999, *ApJ*, 510, 413  
 Leroy, J. L. 1989, in *Dynamics and Structure of Quiescent Solar Prominences*, ed. E. R. Priest (Dordrecht: Kluwer), 77

---

<sup>2</sup>Visit <http://atst.nso.edu/> for a comprehensive description of the project.

- Lin, H. 1995, *ApJ*, 453, 512  
Lin, H. 2004, in preparation  
Lin, H., & Casini, R. 2000, *ApJ*, 542, 528L  
Lin, H., & Rimmele, T. 1999, *ApJ*, 514, 448  
Lin, H., Kuhn, J. R., & Coulter, R. 2004, *ApJ*, in press  
Lin, H., Penn, M. J., & Kuhn, J. R. 1998, *ApJ*, 493, 978  
Lin, H., Penn, M. J., & Tomczyk, S. 2000, *ApJ*, 541, 83L  
Low, B. C., & Lou, Y. Q. 1990, *ApJ*, 352, 343  
Mathew, S. K., Lagg, A., Solanki, S. K., Collados, M., Borrero, J. M., Berdyugina, S., Krupp, N., Woch, J., & Frutiger, C. 2003, *A&A*, 410, 695  
Mickey, D. L. 1973, *ApJ*, 181, L19  
Nagendra, K. N., & Stenflo, J. O. 1999, *Solar Polarization*, Proc. of the 2nd International Workshop on Solar Polarization, ASSL 243 (Dordrecht: Kluwer)  
Rimmele, T. R. 2000, *Proc. SPIE*, 4007, 218  
Roussev, I. I., Gombosi, T. I., Sokolov, I. V., Velli, M., Manchester, W., IV, DeZeeuw, D. L., Liewer, P., Tóth, G., & Luhmann, J. 2003, *ApJ*, 595, L57  
Shchukina, N., & Trujillo Bueno, J. 2003, in *ASP Conf. Ser. Vol. 307, Solar Polarization 3*, ed. J. Trujillo Bueno & J. Sanchez Almeida (San Francisco: ASP)  
Schmid, H. M., Feldt, M., Gratton, R., Joos, F., & Tinbergen, J. 2004, this volume  
Skumanich, A., & Lites, B. W. 1987, *ApJ*, 322, 473  
Skumanich, A., Lites, B. W., Martínez Pillet, V., & Seagrave, P. 1997, *ApJ*, 110, 357  
Smartt, R. 1982, *Proc. SPIE*, 331, 442  
Stenflo, J. O. 1980, *A&A*, 84, 68  
Stenflo, J. O. 1994, *Solar Magnetic Fields—Polarized Radiation Diagnostics* (Dordrecht: Kluwer)  
Stenflo, J. O. 2004, *Reviews in Modern Astronomy*, Vol. 17 (Weinheim: Wiley-VCH).  
Stenflo, J. O., & Nagendra, K. N., eds. 1996, *Solar Polarization*, Proc. First Solar Polarization Workshop (Dordrecht: Kluwer)  
Stenflo, J. O., Twerenbold, D., & Harvey, J. W. 1983a, *A&AS*, 52, 161  
Stenflo, J. O., Twerenbold, D., Harvey, J. W., & Brault, J. W. 1983b, *A&AS*, 54, 505  
Trujillo Bueno, J., Landi Degl’Innocenti, E., Collados, M., Merenda, L., & Manso Sainz, R. 2002, *Nature*, 415, 403  
Trujillo Bueno, J., & Sanchez Almeida, J., eds. 2003, *ASP Conf. Ser. Vol. 307, Solar Polarization Workshop 3* (San Francisco: ASP)  
Westendorp Plaza, C., del Toro Iniesta, J. C., Ruiz Cobo, B., Martínez Pillet, V., Lites, B. W., & Skumanich, A. 1998, *ApJ*, 494, 453  
Westendorp Plaza, C., del Toro Iniesta, J. C., Ruiz Cobo, B., Martínez Pillet, V., Lites, B. W., & Skumanich, A., 2001, *ApJ*, 547, 1130